Apparent Aortic Stiffness in Children With Pulmonary Arterial Hypertension

Existence of Vascular Interdependency?

Michal Schäfer, MSc; D. Dunbar Ivy, MD; Steven H. Abman, MD; Alex J. Barker, PhD; Lorna P. Browne, MD; Brian Fonseca, MD; Vitaly Kheyfets, PhD; Kendall S. Hunter, PhD*; Uyen Truong, MD*

Background—Left ventricular dysfunction, mediated by ventricular interdependence, has been associated with negative outcomes in children with pulmonary arterial hypertension (PAH). Considering the dilation of the pulmonary arteries as a paramount sign of PAH, we hypothesized that the ascending aorta will present signs of apparent stiffness in children with PAH and that this effect may be because of mechanical interaction with the dilated main pulmonary artery (MPA).

Methods and Results—Forty-two children with PAH and 26 age- and size-matched controls underwent comprehensive cardiac magnetic resonance evaluation. Assessment of aortic stiffness was evaluated by measuring pulse wave velocity, aortic strain, and distensibility. Children with PAH had significantly increased pulse wave velocity in the ascending aorta (3.4 versus 2.3 m/s for PAH and controls, respectively; P=0.001) and reduced aortic strain (23% versus 29%; P<0.0001) and distensibility (0.47 versus 0.64%/mm Hg; P=0.02). Indexed MPA diameter correlated with pulse wave velocity (P=0.04) and with aortic strain (P=0.02). The ratio of MPA to aortic size correlated with pulse wave velocity (P=0.0098), strain (P=0.0099), and distensibility (P=0.015). Furthermore, aortic relative area change was associated with left ventricular ejection fraction (P=0.045) and ventricular–vascular coupling ratio (P=0.042).

Conclusions—Pediatric PAH patients have increased apparent ascending aortic stiffness, which was strongly associated with the degree of MPA distension. We speculate that distension of the MPA may play a major role in limiting full aortic expansion during systole, which modulates left ventricular performance and impacts systemic hemodynamics in pediatric PAH. **(*Circ Cardiovasc Imaging*. 2017;10:e005817. DOI: 10.1161/CIRCIMAGING.116.005817.)**

Key Words: aortic stiffness ■ heart rate ■ interdependency ■ pediatric pulmonary hypertension ■ pulse wave analysis

Pediatric pulmonary arterial hypertension (PAH) is a disease associated with high morbidity and mortality.[1–3] Right ventricular (RV) dysfunction serves as an important predictor of PAH severity and outcome in both pediatric and adult populations.[4,5] However, studies of ventricular interdependence have shown that PAH is further complicated by evidence of left ventricular (LV) dysfunction, which may be predictive of poor outcomes in adult PAH populations.[6] Similar findings of critical RV–LV interdependence have been recently recognized in children with PAH,[7,8] further suggesting that altered LV performance can accompany progressive changes in RV function in pediatric PAH as well. However, mechanisms that influence LV performance, such as impaired preload, LV diastolic dysfunction, and other factors, remain incompletely understood.

See Editorial by Quail and Muthurangu
See Clinical Perspective

Previous work has suggested that increased LV afterload because of changes in aortic compliance may impact cardiac function in adults with chronic heart failure.[9] Whether pulmonary artery dilation could mechanically alter apparent aortic stiffness in patients with PAH is not known. Main pulmonary artery (MPA)–aorta interactions may play an even more striking role in the pathophysiology of childhood PAH due in part to the compact mediastinal anatomy in children, especially in the setting of RV dilation and dilated pulmonary arteries.[2,10] However, no prior studies have investigated the impact of PAH-induced MPA dilatation on the proximal aorta, which make close and tight contact with each other within the pericardium.

Received September 12, 2016; accepted December 15, 2016.

From the Division of Cardiology, Heart Institute, Children's Hospital Colorado (M.S., D.D.I., B.F., K.S.H., U.T.), Department of Bioengineering, College of Engineering and Applied Sciences (M.S., D.D.I., V.K., K.S.H., U.T.), Division of Pulmonology, Breathing Institute, Children's Hospital Colorado (S.H.A.), and Department of Radiology, Children's Hospital Colorado (L.P.B.), University of Colorado Denver/Anschutz Medical Campus; and Department of Radiology, Feinberg School of Medicine, Northwestern University, Chicago, IL (A.J.B.).

*Drs Truong and Hunter are co-senior authors.

The Data Supplement is available at http://circimaging.ahajournals.org/lookup/suppl/doi:10.1161/CIRCIMAGING.116.005817/-/DC1.

Correspondence to Michal Schäfer, MSc, Department of Bioengineering, Bioscience 2, Anschutz Medical Campus, 12705 E Montview Ave., Suite 100, Aurora, CO 80045. E-mail michal.schafer@ucdenver.edu

Mechanically induced apparent aortic stiffness because of these vascular interactions could potentially increase LV afterload, further compromising LV function in children with PAH.

Consequently, in this study, we sought to determine whether aortic stiffness is increased in children with PAH and whether changes in indices of aortic stiffness are directly associated with the geometry of the MPA and with LV functional performance. These studies were performed with noninvasive magnetic resonance imaging (MRI) techniques that enable assessment of vascular stiffness, including indices based on measurements of pulse wave velocity (PWV), vascular strain, and distensibility. We hypothesized that (1) the ascending aorta of PAH patients will show signs of vascular stiffness and (2) that increased aortic stiffness will be reflective of pulmonary arterial dimensions and LV performance. Greater understanding of the overall PAH pathophysiology in pediatric patients may assist in development of more comprehensive clinical assessments, including disease severity, changes in function over time, and guidance of specific therapies for this population.

Methods

This study was performed with the approval of the Colorado Multi-Institutional Review Board, and all subjects provided written informed consent. We retrospectively identified consecutive PAH patients seen by the Pulmonary Hypertension Clinic at Children's Hospital Colorado from December 2007 to June 2016, who had comprehensive cardiac magnetic resonance (CMR) performed, which included the use of short-axis stack cine of the ventricles, cine phase-contrast imaging of the ascending aorta, and the MPA. The initial diagnosis of PAH was established after evaluation by our Pulmonary Hypertension Program, which included echocardiograms and a prior cardiac catheterization, according to accepted guidelines.[1] The CMR data sets were selectively chosen to be chronologically closest to either an initial or follow-up cardiac catheterization. The ventricular distress molecules, brain natriuretic peptide (BNP) and N-terminal pro-BNP, were collected at the time of catheterization as indicated by clinical care. We excluded subjects with pulmonary valve or pulmonary arterial stenosis or who had previous surgical intervention on the pulmonary vasculature to focus the study on subjects with native proximal pulmonary vascular conduit anatomy. All control subjects were prospectively recruited through campus advertisement and were included if they did not have any known underlying cardiac, pulmonary, or systemic disease.

CMR Protocol

The acquisition protocol was performed as previously described.[11] A gradient echo ECG–gated sequence was applied to obtain tissue intensity and phase velocity maps using a 1.5 or 3.0 Tesla magnet (Magnetom Avanto, Siemens Medical Solutions, Erlangen, Germany; Ingenia, Philips Medical Systems, Best, The Netherlands). Aortic flow hemodynamic data were acquired using cine phase contrast magnetic resonance imaging (PC-MRI). A single slice covering the ascending aortic plane was chosen to be 1 cm above the sinotubular junction to secure sufficient distance from the aortic root (Figure 1). The acquisition plane for the descending aorta was then ≈3 to 4 cm below the aortic isthmus depending on patient size and age. A typical sequence for free-breathing PC-MRI with Cartesian encoding and retrospective sorting had a temporal resolution of 14 to 28 ms with 15 to 58 phases, echo times of 2.2 to 3.5 ms, matrix 160×256, and flip angle of 25° with 100% of the k-space sampled. Depending on patient size and field of view (128–225×210–360 mm), the cross-sectional pixel resolution was found to be 0.82×0.82 to 1.56×1.56 mm^2 with a slice thickness of 5 mm. Resulting acquisition time varied on heart rate between 1 minute 45 s to 3 minutes. Velocity-encoding values were adjusted according to the maximum velocities encountered during scout sequences to avoid aliasing artifact (typical values ranged from 100 to 200 cm/s).

Standard short-axis images were obtained with coverage of the ventricles from base to apex. Postprocessing analysis of the CMR images was performed using QMass (Medis Medical Imaging Systems; Raleigh, NC), in which volumetric data were manually traced and calculated at end diastole and end systole. Volumetric metrics and ejection fraction were indexed by body surface area values. To include a comprehensive overview of the cardiac and vascular conditions on the systemic side, we also assessed the simplified version of the LV ventricular–vascular coupling ratio based on the CMR-derived volumes, estimated by the ratio of LV end-systolic volume and stroke volume.[12]

Vascular Stiffness and Hemodynamic Parameters

To control for age-related differences in pediatric weight and height, aortic and MPA geometric dimensions for the ascending aorta and MPA were normalized by body surface area for intergroup variation and further generalized linear model regression analysis. Vessel strain was measured by means of relative area change (RAC) defined as the difference between maximum and minimum areas divided by maximum value: $(A_{max}-A_{min})/A_{max}\times100\%$. Distensibility for both aortic segments was then computed as the ratio of RAC and pulse pressure. Additionally, to evaluate systemic vascular properties, we computed aortic capacitance assessed by ratio of LV stroke volume and pulse pressure. Blood pressure values were obtained prior to CMR evaluation using pressure oscillometric technique (Invivo, Model 1400 MRI) either in clinic the day prior or in the MRI suite immediately prior to the study commencement. Flow metrics and patient-specific temporal data required for PWV computation were analyzed from time frame–segmented respective magnitude and phase contrast images for both aortic segments, as previously described (Matlab Program; Mathworks, Inc., Natick, MA).[13,14] Specifically, each temporal phase was segmented using semiautomatic level-set method (Segment, Medviso), where constructed algorithm applies active contour model, which tracks the edges of the vessel wall initialized by a manual delineation in 1 time frame. The following parameters were sampled from patient-specific flow waves: maximum flow (Q_{max}), maximum velocity (V_{max}), maximum wall shear stress (WSS_{max}), and oscillatory shear index, all computed and analyzed as described previously.[13,15]

PWV was measured as a determinant of aortic stiffness. We used the dQ/dA method, previously recognized as a sensitive PWV measure by incorporating temporal variation in flow and luminal area data sets.[16] The PWV was computed as a function of the variation ratio of through-plane aortic flow and cross-sectional aortic area, that is, the slope of the flow–area relation during early systole. The PWV was then calculated from the flow–area plots by using a linear regressional model to create a line fitted to the flow–area curve at early systole as described previously (see Figure 2). This technique describes segment-specific evaluation of aortic stiffness, rather than global aortic stiffness. Furthermore, this method overcomes potential spatiotemporal limitations typically associated with standard travel time of flow PWV calculation, which are of high risk in a pediatric population.[17,18]

Statistical Analysis

Analyses were performed in SAS (version 9.4 or higher; SAS Institute, Cary, NC). Variables were checked for the distributional assumption of normality using normal plots, in addition to Kolmogorov–Smirnov and Shapiro Wilks tests. Variables that were positively skewed (eg, PWV, RAC, and BNP) were natural log-transformed for the analyses. Demographic and clinical characteristics among children with and without PAH were compared using student t test for normally distributed continuous variables and χ^2 for categorical variables. Additional group comparisons were performed using Kruskal–Wallis test between the PAH-specific World Health Organization functional classes. Generalized linear regression models were used to examine association between aortic stiffness (PWV, RAC, and distensibility) and MPA geometric parameters and risk factors associated with pediatric PAH (LV ejection fraction and ventricular–vascular coupling ratio, mean pulmonary artery pressure, pulmonary vascular resistance index, N-terminal pro-BNP, BNP) adjusted for age and sex. Significance was based on an α level of 0.05.

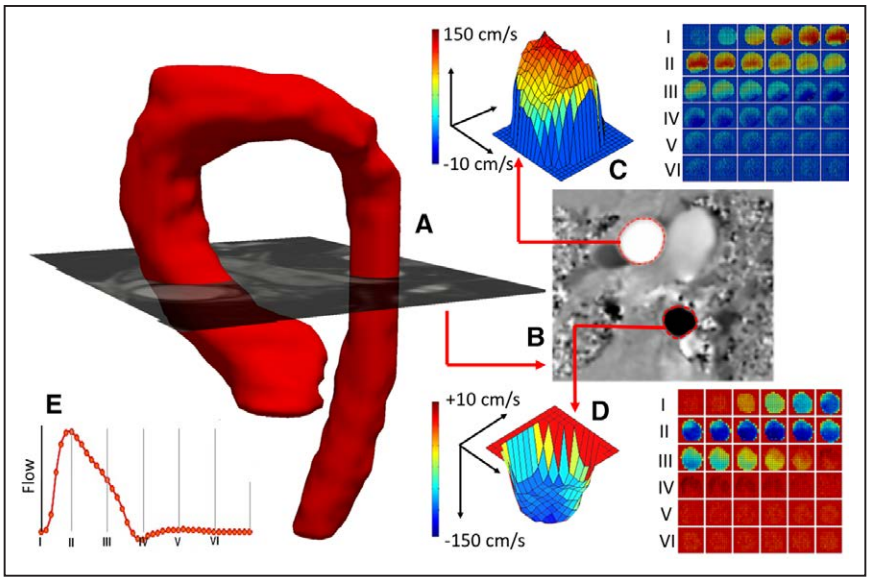

Figure 1. A, Magnetic resonance angiography (MRA) reconstructed aorta with superimposed phase contrast magnetic resonance imaging magnitude image plane depicting the flow hemodynamic computation locations. **B**, Corresponding phase image with segmented ascending and descending aortic lumens for flow hemodynamic quantification (**C** and **D**) and reconstructed flow-wave form (**E**). MRI indicates magnetic resonance imaging.

Results

Demographic and basic hemodynamic measurements are summarized in Table 1. We identified 42 PAH patients and recruited 26 controls with equivalent age and sex distributions. PAH children patients presented significantly decreased body mass index percentile and body surface area when compared with the controls. The average time between the right heart catheterization and CMR acquisition was 302 days (range 0–401 days). The average mean pulmonary artery pressure and pulmonary vascular resistance index from the chronologically closest catheterization were 44±14 mm Hg and 9±7 Wood units×m^2, respectively. There were 18 subjects with idiopathic PAH (IPAH), 22 children with PAH associated with congenital heart disease (CHD-PAH), and 2 patients with PAH associated with bronchopulmonary dysplasia. CHD-PAH pathogeneses included atrial septal defects (13; 30.9%), ventricular septal defects (5; 11.9%), and patent ductus arteriosus (5; 11.9%, 2 postligation repair). Furthermore, 5 PAH patients had a shunt present at the time of CMR evaluation (2 with left-to-right shunting). Five PAH patients and 2 controls were excluded from the vascular analysis because of the close proximity of the acquisition plane to aortic root, disabling vessel wall segmentation.

As anticipated, children with PAH had significantly increased RV end-diastolic (138 versus 92 mL/m^2; P=0.0005) and end-systolic volumes (84 versus 41 mL/m^2; P=0.0008) along with reduced RV ejection fraction (44% versus 58%; P=0.0012). Although no significant variation existed between considered groups between LV volumetric indices (end diastolic, end systolic, and stroke volume), children with PAH presented significantly decreased LV ejection fraction (53% versus 58%; P=0.0231). Systemic pressure metrics did not reveal any significant variability between PAH and control groups. Data from the PAH group showed significantly increased indexed MPA diameter (2.68 versus 1.6 cm/m^2; P<0.0001) and increased MPA/aortic diameter ratio measured at systole (1.42 versus 1.07; P<0.0001).

PC-MRI-derived flow data for both aortic segments are summarized in Table 2. All vascular stiffness measures were significantly different between PAH and control groups in the ascending aorta. PWV (cm/s) was significantly increased in PAH children (3.4 versus 2.3; P=0.0014), indicative of increased ascending aortic stiffness in this disease group. Both geometric-related metrics in the ascending aorta—RAC (%) and distensibility (%/mm Hg)—were significantly decreased in the PAH group (23 versus 29, P<0.0001; and 0.47 versus 0.64, P=0.0242, respectively). Interestingly, these reductions in strain metrics occurred in parallel with decreased maximum aortic area in PAH patients (4.5 versus 5.3 cm^2; P=0.0282), whereas the minimal aortic area was similar between both considered groups. The aortic capacitance (stroke volume/pulse pressure; mL/mm Hg) was similar among considered

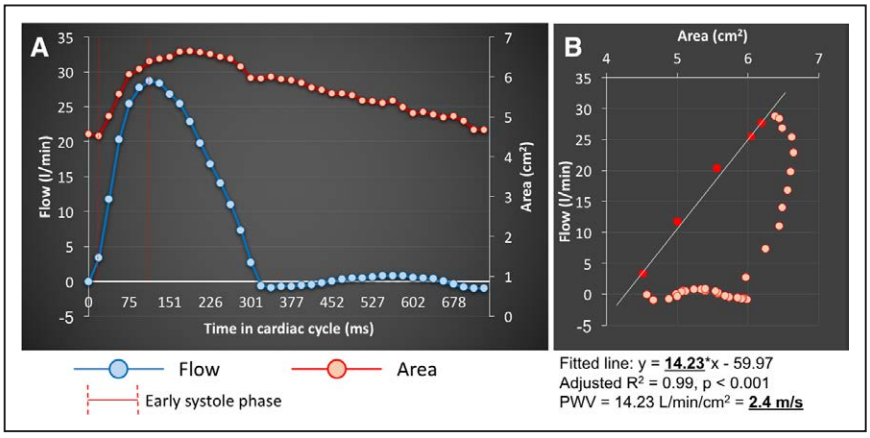

Figure 2. The pulse wave velocity (PWV) computation algorithm. **A**) The PWV was calculated from the flow–area plots by using a linear regressional model to create a line fitted to the flow–area curve (**B**) at early systole. The calculated model coefficients then served for computation of PWV.

Table 1. Demographics and Hemodynamics Measurements

	PAH (n=42)	Control (n=26)	*P* Value
Age, y	14.6±4.6	15.1±3.2	0.6110
Sex, female (%)	23 (54.7)	13 (50.0)	0.7956
BMI	19.6±5.2	21.4±3.1	0.0934
BMI percentile	42.3±30.9	60.8±22.7	0.0082
BSA, m^2	1.40±0.38	1.58±0.27	0.0313
IPAH, n (%)	18 (42.8)		
CHD-PAH	22 (42.3)		
ASD	13 (30.9)		
VSD	5 (11.9)		
PDA	5 (11.9)		
BPD	2 (4.7)		
Systolic BP, mm Hg	106±12	112±9	0.1338
Diastolic BP, mm Hg	61±7	64±6	0.1683
Pulse pressure, mm Hg	45±11	46±10	0.8161
Shunt present at CMR evaluation	5 (11.9)		
World Health Organization functional classification			
WHO-FC I	7 (16.6)		
WHO-FC II	17 (40.4)		
WHO-FC III	12 (28.5)		
WHO-FC IV	6 (14.2)		
Cardiac catheterization			
mPAP, mm Hg	44±17		
PVRI, WU/m^2	9±7		
PAWP, mm Hg	9±2		
NT-proBNP, pg/mL	156 (73–445)		
BNP, pg/mL	42 (15–106)		
CMR hemodynamics			
LV end-diastolic volume,* mL/m^2	93±34	89±18	0.8567
LV end systolic,* mL/m^2	41±17	39±15	0.6614
LV stroke volume,* mL/m^2	48±16	51±9	0.3623
LV ejection fraction, %	53±10	58±4	0.0231
LV VVCR–ESV/SV	0.99±0.63	0.75±0.17	0.0986
Cardiac index,* L/min per m^2	3.9±0.9	3.8±0.9	0.7198
Heart rate, bpm	79±16	72±15	0.1254
RV end-diastolic volume,* mL/m^2	138±73	92±14	0.0005
RV end-systolic volume,* mL/m^2	84±73	41±9	0.0008
RV stroke volume,* mL	53±14	51±10	0.5928
RV ejection fraction, %	44±14	58±11	0.0012
MPA diameter,* cm/m^2	2.48 (2.09–2.93)	1.61 (1.54–1.79)	<0.0001
Aortic diameter,* cm/m^2	1.63 (1.44–1.94)	1.60 (1.49–1.83)	0.9792
MPA/aorta size ratio	1.42 (1.23–1.67)	1.07 (0.99–1.09)	<0.0001

Data are expressed as averages±SD or medians with interquantile range. ASD indicates atrial septal defect; BMI, body mass index; BNP, brain natriuretic peptide; BP, blood pressure; BPD, bronchopulmonary dysplasia; BSA, body surface area; CHD-PAH, pulmonary arterial hypertension associated with congenital heart disease; CMR, cardiac magnetic resonance; ESV, end-systolic volume; IPAH, idiopathic pulmonary arterial hypertension; LV, left ventricle; MPA, main pulmonary artery; mPAP, mean pulmonary artery pressure; NT-proBNP, N-terminal pro-brain natriuretic peptide; PAH, pulmonary arterial hypertension; PAWP, pulmonary arterial wedge pressure; PDA, patent ductus arteries; PVRI, pulmonary vascular resistance index; RV, right ventricle; SV, stroke volume; VSD, ventricular septal defect; VVCR, ventricular-vascular coupling ratio; and WHO-FC, World Health Organization functional classification.

*Metrics are normalized by BSA.

groups (1.51 versus 1.81; *P*=0.2705). Both shear hemodynamic metrics WSS_{max} and oscillatory shear index failed to reveal any significant variability, as well as the shear theoretical determinants V_{max} and Q_{max}. No changes in considered stiffness metrics were observed in the descending aorta.

To exclude the potential mechanical changes associated with surgical intervention and pericardial manipulation, we excluded those with thoracic surgical history (n=6) from aortic stiffness comparative analysis and observed in the resulting subset minimal parametric changes in all considered stiffness metrics (PWV: 3.6 versus 2.3, *P*=0.0091; RAC: 20.6 versus 29.2, *P*<0.0001; distensibility: 0.49 versus 0.64, *P*=0.0381; capacitance: 1.56 versus 1.81, *P*=0.2816). Again in the subset, both shear hemodynamic metrics WSS_{max} and oscillatory shear

Table 2. Vascular Hemodynamics

	Ascending Aorta		Descending Aorta	
	PAH	Control	PAH	Control
PWV, m/s	3.4 (3.1–4.0)*	2.3 (1.8–3.4)	3.3 (2.8–3.9)	3.1 (2.6–3.6)
Q_{max}, L/min	18.0±6.7	21.0±5.2	10.4±4.6	12.1±2.8
V_{max}, cm/s	113±27	117±22	107±25	102±45
A_{max}, cm^2	4.5±1.7*	5.3±1.0	2.8±0.9	3.0±0.7
A_{min}, cm^2	3.5±1.4	3.7±0.7	1.9±0.7	2.2±0.5
RAC, %	23 (16–25)†	29 (26–31)	23 (21–27)	25 (21–29)
Distensibility, %/mm Hg	0.47±0.26*	0.64±0.21	0.56±0.28	0.62±0.26
Capacitance, mL/mm Hg	1.51±0.27	1.81±0.73	…	…
WSS_{max}, dyne/cm^2	9.5±3.6	8.5±2.4	10.7±2.9	10.5±2.4
OSI	0.04±0.04	0.03±0.03	0.03±0.04*	0.01±0.00

Data are expressed as averages±SD or medians with interquantile range. OSI indicates oscillatory shear index; PAH, pulmonary arterial hypertension; PWV, pulse wave velocity; RAC, relative area change; V_{max}, maximum velocity; and WSS_{max}, systolic wall shear stress.

*Significant differences (*P*<0.05).

†*P*<0.001.

index measured in the ascending aorta failed to reveal any significant variability, as well as the shear theoretical determinants V_{max} and Q_{max}. All considered stiffness and flow hemodynamic metrics measured in the descending aorta did not reveal any significant difference between control and the PAH subgroup, with exception of oscillatory shear index, which was significantly increased in PAH children (0.03 versus 0.01; P=0.0010).

To investigate the potential relationship between the disease severity and aortic stiffness, we looked for variability among the PAH groups by World Health Organization functional class with respect to aortic strain. Although patients with worse World Health Organization functional class tended toward reduced aortic strain, no intergroup significant difference existed between World Health Organization functional class groups (P=0.171) as shown in Figure 3.

Furthermore, no differences were found in stiffness and hemodynamic metrics between IPAH and CHD-PAH groups. We performed subgroup analysis of ascending aortic stiffness measures to assess the potential variability between IPAH and CHD-PAH groups. Although there was no difference in stiffness metrics between the 2 PAH groups, both groups had decreased RAC and increased PWV when compared with the controls (Figure 4). Distensibility and capacitance were not different between groups. Normalized MPA diameter values were increased for both CHD-PAH and IPAH when compared with the controls but were not different between the PAH groups (Figure 5). Similarly, MPA to ascending aortic size ratios were significantly increased for both CHD-PAH and IPAH in comparison with the controls but were not different between PAH cohorts.

A summary of generalized linear regression models between vascular stiffness metrics and standard geometric metrics and PAH risk factors are depicted in Table 3 (reported as beta±standard error). All reported models were adjusted for sex and age. Significant positive association existed between ln PWV and indexed MPA diameter (0.416±0.196; P=0.0400) and between ln PWV and MPA/aortic size ratio (0.611±0.226; P=0.0098). Concurrently, ln RAC correlated negatively with MPA diameter (−0.344±0.248; P=0.0285) and MPA/aortic ratio (−0.468±0.174; P=0.0099). Additionally, ln RAC correlated positively with LV ejection fraction (0.009±0.004; P=0.0456) and negatively with LV ventricular–vascular coupling ratio (−0.159±0.076; P=0.0424). Finally, aortic distensibility correlated in negative fashion with MPA/aortic size ratio (−0.006±0.002; P=0.0150).

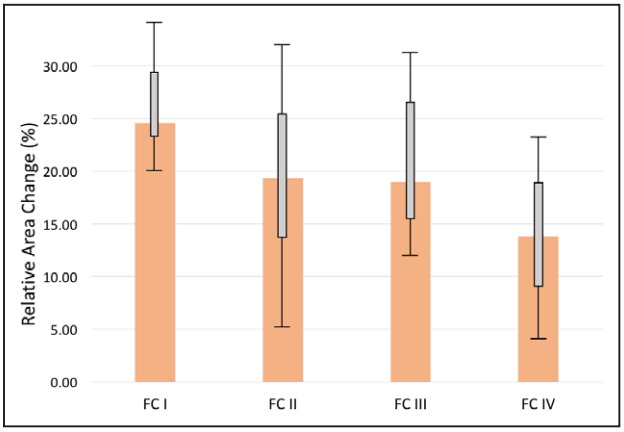

Figure 3. The median values and corresponding interquartile ranges (IQRs) of aortic area strain among specific World Health Organization (WHO) functional classes (FC). There was no observed intergroup variability between WHO-FC with respect to the most significantly altered measured stiffness metric—relative area change (RAC; P=0.171; Kruskal–Wallis).

Conventional PAH risk factor variables (mean pulmonary artery pressure, pulmonary vascular resistance index, N-terminal pro-BNP, and BNP) failed to reveal any significant correlations with indices of aortic stiffness (PWV, RAC, and distensibility). However, significant positive correlations existed between the MPA/aortic size ratio and catheterization-derived mean pulmonary artery pressure (0.008±0.002; P=0.0014) and pulmonary vascular resistance index (0.025±0.007; P=0.0019; Figure in the Data Supplement). To investigate the relationship between MPA size and LV systolic function, we correlated MPA/aortic size ratio directly with LVEF and LV ventricular–vascular coupling ratio (Figure 6). We found a significant negative linear relationship between MPA/aortic ratios and LVEF (−8.830±3.012; P=0.0005) and positive associations with LV ventricular–vascular coupling (0.323±0.131; P=0.0169).

Discussion

In this study, we have shown that children with PAH have increased apparent aortic stiffness, which was strongly associated with increased MPA size. To our knowledge, this is a first report of reduced functional systemic vascular performance in any PAH population combining evidence from 3 well-accepted indices of stiffness. Furthermore, we found that decreased aortic strain measured by means of RAC is significantly associated with lower LV ejection fraction and higher ventricular–vascular coupling ratio. Therefore, increased apparent aortic stiffness, which contributes to systemic afterload, is associated with negative functional consequences in an already compromised LV. Because of the inherent nature of the PAH pathophysiology, past studies in pediatric PAH have focused solely on metrics of RV function and pulmonary vascular stiffness, either in separate or combined fashion.[11,15,19,20] More recently, the increasingly recognized concept of ventricular interdependency has been shown to have important mechanical effects on the LV performance in both adult and pediatric PAH populations.[6,8,21] Although the mean LV ejection fraction of our PAH cohort was close to the lower limit of normal, the statistically significant difference point to a compromised LV systolic function as observed in previous multicenter pediatric study.[22] Importantly, in adult and pediatric PAH populations, compromised LV function because of ventricular interdependency was shown to have a clinically prognostic potential.[6,7] This newly observed effect of potentially existing vascular interdependency might then play important role in overall cardiovascular performance in children with PAH.

Presence of Vascular Interdependency

Although MPA stiffness has been successfully associated with metrics of RV function and hemodynamics, such as flow and shear stress, the reduced aortic distensibility seems to be driven primarily by regional physical effects. Our results indicate that increased MPA size, absolute and indexed to aortic diameter, is associated with increased regional changes in apparent aortic stiffness. All considered stiffness metrics take into account extrinsic geometric vascular properties, and in particular, depressed

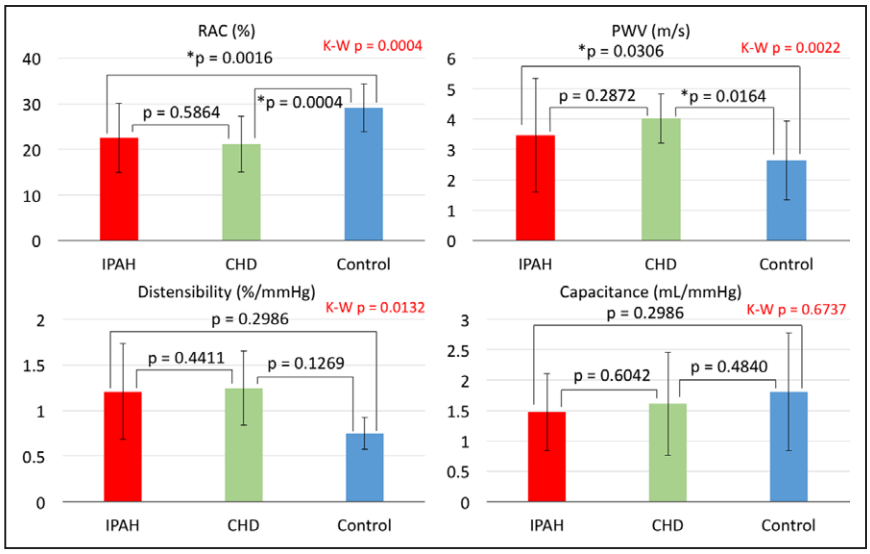

Figure 4. The subanalysis of ascending aortic stiffness metrics between pulmonary arterial hypertension associated with congenital heart disease (CHD-PAH), idiopathic pulmonary arterial hypertension (IPAH), and control groups. IPAH and CHD-PAH groups did not present any significant variability in any considered aortic stiffness metrics. However, in the case of relative area change (RAC) and pulse wave velocity (PWV) representing local aortic stiffness, both PAH groups showed significant differences from the control group. No variability existed among considered groups in distensibility and capacitance assessing rather global aortic stiffness. K-W indicates Kruskal–Wallis.

maximum aortic size seems to be responsible for the majority of altered variables within the PAH group. We speculate that PAH-related MPA dilatation mechanically impairs the ability of regions of the ascending aorta to fully expand during systole. Further evidence supporting this potential mechanism can be seen from the aortic wall deformation analysis generated from a vascular segmentation process, as shown in Figure 7. From the representative PAH case, it seems that ascending aorta has more room for expansion in the directions toward the vena cava and right atrium, whereas the range of motion tends to be limited where the aorta is in contact with the MPA. Conversely, the depicted control case shows uniform circumferential expansion. However, standardized comprehensive wall deformation analysis across larger data sets would be required to fully understand potential mechanical suppressing effects arising from the distended MPA.

The argument of locally driven vascular interdependency is also supported by the fact that the stiffness metrics analyzed in the descending aorta failed to show any variability between PAH and control groups. Furthermore, PAH subpopulations considered in this study, CHD-PAH and IPAH, failed to present major variability in the apparent stiffness metrics, yet have major variability differences from control group. Per our results, severity of MPA dilation seems to be uniform among the PAH subgroups (IPAH and CHD-PAH), with similar impact on ascending aortic expansion and overall apparent stiffness. Thus, aortic stiffening does not seem to be a global phenomenon, which might be expected if it were because of other causes, such as pressure overload or systemic inflammation. The descending aorta is in close proximity to the pulmonary vasculature only at the region of the subclavian ligament bypassing the left pulmonary artery. Because our acquisition plane for descending aortic analysis was positioned further distally, we speculate that this particular aortic segment was free from constriction that is potentially caused by the pulmonary vasculature and, therefore, did not reveal any signs of aortic stiffness.

Additional mechanisms might play role in the increased aortic stiffness in PAH. Pulmonary vascular remodeling, including changes in the large proximal vessels, has been associated with the PAH pathobiology, which may be related to increased inflammation because of increased hemodynamic stress.[2,23,24] Although PAH-associated inflammatory processes have been previously associated with pulmonary vascular remodeling, changes in tissue remodeling in the aorta has not been examined. Finally, aortic shear hemodynamic metrics, commonly associated with flow-mediated endothelial mechanotransduction remodeling, were not altered between the PAH and control groups.[25,26] However, future longitudinal studies involving thorough analysis of known potential inflammatory vascular remodeling mediators may further explore the potential for tissue remodeling within the aorta in the setting of progressive PAH.

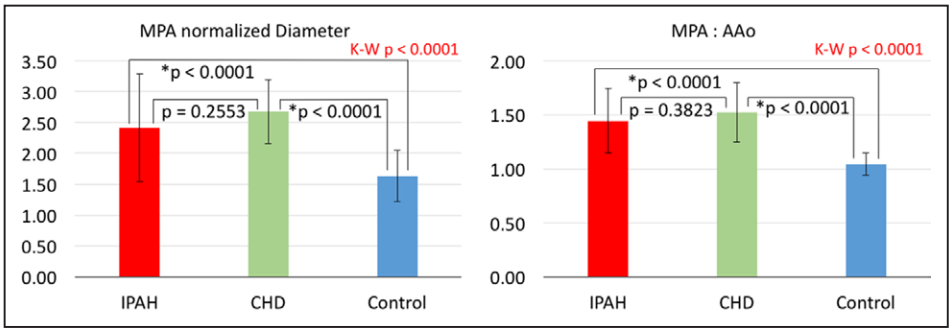

Figure 5. The subanalysis of vessel size metrics between pulmonary arterial hypertension associated with congenital heart disease (CHD-PAH), idiopathic pulmonary arterial hypertension (IPAH), and control groups. Both main pulmonary artery (MPA)–normalized diameter and MPA to ascending aortic ratio revealed significantly higher average values for both considered PAH groups when compared with controls. However, no differences were observed between PAH groups. K-W indicates Kruskal–Wallis.

Table 3. Associations With Ascending Aortic Stiffness

	ln PWV, m/s	ln RAC, %	Distensibility, %/mm Hg
MPA diameter	0.416±0.196 (0.0400)*	−0.344±0.248 (0.0285)*	−0.205±0.121 (0.0989)
MPA/aorta ratio	0.611±0.226 (0.0098)*	−0.468±0.174 (0.0099)*	−0.006±0.002 (0.0150)*
LVEF	0.004±0.009 (0.6870)	0.009±0.004 (0.0456)*	0.005±0.002 (0.1643)
LV VVCR (ESV/SV)	0.048±0.112 (0.6652)	−0.159±0.076 (0.0424)*	−0.077±0.049 (0.1240)
mPAP	−0.005±0.003 (0.2138)	−0.010±0.005 (0.0848)	0.001±0.002 (0.9471)
PVRI	0.005±0.004 (0.2139)	−0.011±0.015 (0.4491)	0.010±0.006 (0.1408)
NT-proBNP	−0.002±0.048 (0.9623)	−0.121±0.068 (0.0856)	−0.107±0.086 (0.2225)
BNP	−0.020±0.073 (0.7821)	−0.182±0.097 (0.0686)	−0.171±0.122 (0.1702)

Data are beta coefficients±SEM (*P* values). Significant ($P<0.05$) associations are in bold. All considered models were adjusted for age and sex. BNP indicates brain natriuretic peptide; ESV, end-systolic volume; LVEF, left ventricular ejection fraction; MPA, main pulmonary artery; mPAP, mean pulmonary artery pressure; NT-proBNP, N-terminal pro-brain natriuretic peptide; PVRI, pulmonary vascular resistance index; PWV, pulse wave velocity; RAC, relative area change; and VVCR, ventricular-vascular coupling ratio.

*Significant differences ($P<0.05$).

Aortic Strain and LV Performance Relationship

Although all stiffness metrics showed significant differences between PAH and control groups, only RAC correlated with LV ejection fraction and LV-specific ventricular–vascular coupling ratio. The RAC, unlike PWV, distensibility, and capacitance, is a pure geometric parameter that solely assesses 2-dimensional (area) strain. As a result, RAC can be more reflective of anatomically constraining structures that may reduce vessel expansion to maximum area.[27] On the other hand, PWV, distensibility, and capacitance take into account flow, pressure, and volume changes, respectively, and are then less geometry dependent and can reflect more on true vessel mechanical constitutive changes.[28,29] Indeed, RAC showed the most significant differences from all considered stiffness metrics in parallel with reduced maximum area in the PAH group. Conversely, peak flow (Q_{max}), pressure, and volume metrics determining PWV and distensibility, respectively, were not different between control and PAH groups. Additionally, aortic distensibility and capacitance considered to be reflective of global aortic stiffness failed to show any significant intergroup variability, suggesting that reduced apparent ascending aortic stiffness is driven by a local mechanical factors. The local nature of the dilated MPA impinging on the ascending aortic conduit would be most precisely quantified via complete impedance spectra analysis, enabling investigation of local compression–arterial impedance. However, the collection of the impedance spectra in the systemic circulation in this patient population is problematic because of clinical–ethical reasons. Future studies will focus on comprehensive aortic 4D-Flow MRI to assess the qualitative flow patterns along with the energy loss index across the ascending aorta to fully investigate the constriction mechanism.

Therefore, we speculate that changes in apparent ascending aortic stiffness were purely because of anatomic compression by the enlarged, neighboring MPA reflected in the most sensitive way by RAC analysis. The compression of ascending aorta within the pericardial limit by MPA seems to further increase LV afterload, as reflected by association with the LV ejection fraction. Finally, the correlation between RAC and LV ventricular–vascular coupling ratio implies that compromised expansion of proximal aorta might have negative afterload-dependent effects on LV performance in pediatric PAH. We also found direct correlation between the MPA to ascending aortic size ratio with LV ejection fraction and ventricular–vascular coupling ratio. Overall, we further speculate that vascular interdependency might add to PAH-induced pathophysiology and add to worsening prognosis associated with LV dysfunction in PAH (Figure 8).

Study Limitations

One potential limitation of our study is that the mean time between PC-MRI acquisition and catheterization is variable within our PAH group. We also recognize that some patients underwent the catheterization under anesthesia while being awake for the CMR, which potentially can alter the

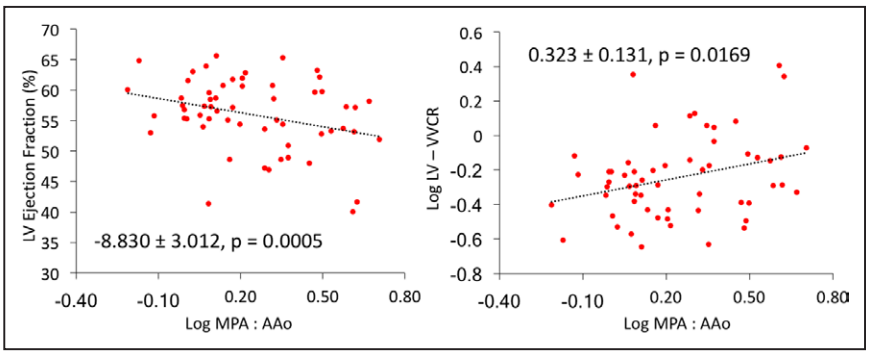

Figure 6. Associations between main pulmonary artery (MPA)/ascending aorta size ratio and left ventricular (LV) ejection fraction (**left**) and LV ventricular–vascular coupling ratio (VVCR; **right**). Both trends are suggestive of negative MPA expansion effect on the ascending aorta, resulting in increased LV afterload. Both models are adjusted for age and sex.

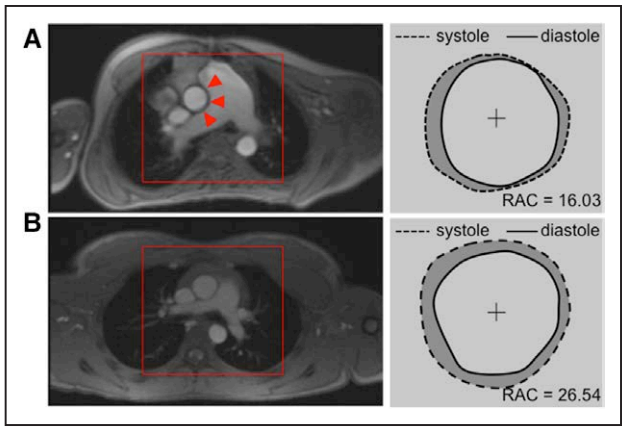

Figure 7. Pulmonary artery impingement on aorta. **A**, On this representative pediatric pulmonary arterial hypertension (PAH) patient, one can immediately notice a severely dilated main pulmonary artery (MPA) impinging on the ascending aorta. Wall deformation analysis from segmented PC-MRI magnitude images shows reduced range of motion along the aortic–MPA interface highlighted by red triangles. **B**, Conversely, representative control subject reveals size proportional vessel and uniform aortic expansion along the central axis. MRI indicates magnetic resonance imaging; and RAC, relative area change.

hemodynamic state. However, this is unavoidable because vast majority of pediatric catheterizations at our institution is performed under general anesthesia, and within this study, only 6 PAH patients (<8 years) required anesthesia. Future studies will involve synchronized catheterization and noninvasive imaging studies, including echocardiography and 4-dimensional flow MRI, to qualitatively assess the sensitive flow disturbances associated with stiffness-compromised vessels.

PWV assessed by flow-area method works under major assumption of reflection-less free pulse wave in the evaluated vessel region. By evaluating PWV in the ascending and proximal thoracic aorta, the planes of evaluation should be sufficiently distant from resistant arterioles, considered to be the major source of impeding pulse wave. Additionally, we did not observe major reflection from the primary aortic branches usually presented as a major reduction in dQ/dA at the end of initial systole phase. However, this PWV computation method is highly sensitive to segmentation errors (through-plane motion, signal loss at high flow rates, nonuniform flow wave etc.).[16,30]

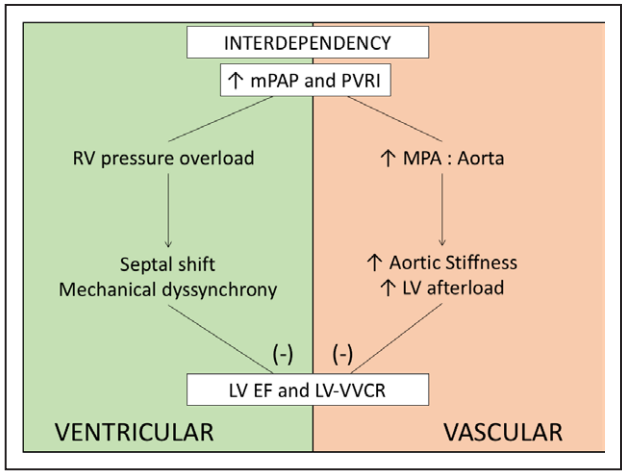

Figure 8. Proposed schematic of overall interdependency phenomenon in pediatric pulmonary arterial hypertension (PAH). Paramount signs of PAH, increased mean pulmonary artery pressure (mPAP), and pulmonary vascular resistance index (PVRI) seems to mechanically affect left ventricular (LV) functionality via both proximal pulmonary vascular and ventricular interdependency. EF indicates ejection fraction; MPA, main pulmonary artery; RV, right ventricle; and VVCR, ventricular–vascular coupling ratio.

Another limitation of this study is that included subjects underwent PC-MRI acquisition on 2 different scanning systems. Ideally, the same acquisition sequence and vendor system would have been applied to every subject. Furthermore, given that both systems operate on different magnetic field strengths, intersystem variability is an important consideration. However, the variable field strength has been shown previously to not alter the flow hemodynamic measurements.[31] The heterogeneity of PAH pathogenesis and the body mass index difference between the control and PAH population may have also compromised the overall results.

Conclusions

Pediatric PAH patients have a focal increase in the apparent ascending aortic stiffness as assessed by CMR studies. The apparent aortic stiffness is strongly associated with the degree of distension of the MPA. We speculate that distension of the MPA contributes to aortic stiffness because of its role in limiting full aortic expansion during systole within a restricted space of the thoracic cavity. We propose that in addition to ventricular interdependency, vascular interdependency of the MPA and aorta can potentially have negative effects on LV performance in pediatric PAH, which is primarily because of the mechanical effects of MPA distension.

Sources of Funding

This research was supported in part by the Actelion ENTELLIGENCE Grant, Children's Hospital Colorado Research Scholar Award, Colorado Clinical Translation Sciences Institute Maternal and Child Pilot Grant, The Frederick and Margaret L. Weyerhaeuser Foundation, The Jayden de Luca Foundation, NIH grants R01HL114753, U01HL121518, NHLBI U01 HL12118, NHLBI RO1 HL085703, NHLBI RO1 HL68702, K25-HL094749, and by NIH/NCATS Colorado CTSA Grant Number UL1 TR001082.

Disclosures

None.

References

1. Abman SH, Hansmann G, Archer SL, Ivy DD, Adatia I, Chung WK, Hanna BD, Rosenzweig EB, Raj JU, Cornfield D, Stenmark KR, Steinhorn R, Thébaud B, Fineman JR, Kuehne T, Feinstein JA, Friedberg MK, Earing M, Barst RJ, Keller RL, Kinsella JP, Mullen M, Deterding R, Kulik T, Mallory G, Humpl T, Wessel DL; American Heart Association Council on Cardiopulmonary, Critical Care, Perioperative and Resuscitation; Council on Clinical Cardiology; Council on Cardiovascular Disease in the Young; Council on Cardiovascular Radiology and Intervention; Council on Cardiovascular Surgery and Anesthesia; and the American Thoracic Society. Pediatric pulmonary hypertension: Guidelines From the American Heart Association and American Thoracic Society. *Circulation*. 2015;132:2037–2099. doi: 10.1161/CIR.0000000000000329.
2. Ivy DD, Abman SH, Barst RJ, Berger RM, Bonnet D, Fleming TR, Haworth SG, Raj JU, Rosenzweig EB, Schulze Neick I, Steinhorn RH, Beghetti M. Pediatric pulmonary hypertension. *J Am Coll Cardiol*. 2013;62(25 suppl):D117–D126. doi: 10.1016/j.jacc.2013.10.028.
3. Zijlstra WM, Douwes JM, Rosenzweig EB, Schokker S, Krishnan U, Roofthooft MT, Miller-Reed K, Hillege HL, Ivy DD, Berger RM. Survival

differences in pediatric pulmonary arterial hypertension: clues to a better understanding of outcome and optimal treatment strategies. *J Am Coll Cardiol*. 2014;63:2159–2169. doi: 10.1016/j.jacc.2014.02.575.
4. Vonk-Noordegraaf A, Haddad F, Chin KM, Forfia PR, Kawut SM, Lumens J, Naeije R, Newman J, Oudiz RJ, Provencher S, Torbicki A, Voelkel NF, Hassoun PM. Right heart adaptation to pulmonary arterial hypertension: physiology and pathobiology. *J Am Coll Cardiol*. 2013;62(25 suppl):D22–D33. doi: 10.1016/j.jacc.2013.10.027.
5. Hopper RK, Abman SH, Ivy DD. Persistent challenges in pediatric pulmonary hypertension. *Chest*. 2016;150:226–236. doi: 10.1016/j.chest.2016.01.007.
6. Hardegree EL, Sachdev A, Fenstad ER, Villarraga HR, Frantz RP, McGoon MD, Oh JK, Ammash NM, Connolly HM, Eidem BW, Pellikka PA, Kane GC. Impaired left ventricular mechanics in pulmonary arterial hypertension: identification of a cohort at high risk. *Circ Heart Fail*. 2013;6:748–755. doi: 10.1161/CIRCHEARTFAILURE.112.000098.
7. Moledina S, Pandya B, Bartsota M, Mortensen KH, McMillan M, Quyam S, Taylor AM, Haworth SG, Schulze-Neick I, Muthurangu V. Prognostic significance of cardiac magnetic resonance imaging in children with pulmonary hypertension. *Circ Cardiovasc Imaging*. 2013;6:407–414. doi: 10.1161/CIRCIMAGING.112.000082.
8. Burkett DA, Slorach C, Patel SS, Redington AN, Ivy DD, Mertens L, Younoszai AK, Friedberg MK. Left ventricular myocardial function in children with pulmonary hypertension: relation to right ventricular performance and hemodynamics. *Circ Cardiovasc Imaging*. 2015;8:e003260. doi: 10.1161/CIRCIMAGING.115.003260.
9. Chantler PD, Lakatta EG, Najjar SS. Arterial-ventricular coupling: mechanistic insights into cardiovascular performance at rest and during exercise. *J Appl Physiol (1985)*. 2008;105:1342–1351. doi: 10.1152/japplphysiol.90600.2008.
10. Jone PN, Ivy DD. Echocardiography in pediatric pulmonary hypertension. *Front Pediatr*. 2014;2:124. doi: 10.3389/fped.2014.00124.
11. Truong U, Fonseca B, Dunning J, Burgett S, Lanning C, Ivy DD, Shandas R, Hunter K, Barker AJ. Wall shear stress measured by phase contrast cardiovascular magnetic resonance in children and adolescents with pulmonary arterial hypertension. *J Cardiovasc Magn Reson*. 2013;15:81. doi: 10.1186/1532-429X-15-81.
12. Sanz J, García-Alvarez A, Fernández-Friera L, Nair A, Mirelis JG, Sawit ST, Pinney S, Fuster V. Right ventriculo-arterial coupling in pulmonary hypertension: a magnetic resonance study. *Heart*. 2012;98:238–243. doi: 10.1136/heartjnl-2011-300462.
13. Barker AJ, Lanning C, Shandas R. Quantification of hemodynamic wall shear stress in patients with bicuspid aortic valve using phase-contrast MRI. *Ann Biomed Eng*. 2010;38:788–800. doi: 10.1007/s10439-009-9854-3.
14. Heiberg E, Sjögren J, Ugander M, Carlsson M, Engblom H, Arheden H. Design and validation of Segment–freely available software for cardiovascular image analysis. *BMC Med Imaging*. 2010;10:1. doi: 10.1186/1471-2342-10-1.
15. Schäfer M, Ivy DD, Barker AJ, Kheyfets V, Shandas R, Abman SH, Hunter KS, Truong U. Characterization of CMR-derived haemodynamic data in children with pulmonary arterial hypertension. *Eur Hear J Cardiovasc Imaging*. 2016;jew152.
16. Herold V, Parczyk M, Mörchel P, Ziener CH, Klug G, Bauer WR, Rommel E, Jakob PM. *In vivo* measurement of local aortic pulse-wave velocity in mice with MR microscopy at 17.6 Tesla. *Magn Reson Med*. 2009;61:1293–1299. doi: 10.1002/mrm.21957.
17. Wentland AL, Grist TM, Wieben O. Review of MRI-based measurements of pulse wave velocity: a biomarker of arterial stiffness. *Cardiovasc Diagn Ther*. 2014;4:193–206. doi: 10.3978/j.issn.2223-3652.2014.03.04.
18. Forouzan O, Warczytowa J, Wieben O, François CJ, Chesler NC. Noninvasive measurement using cardiovascular magnetic resonance of changes in pulmonary artery stiffness with exercise. *J Cardiovasc Magn Reson*. 2015;17:109. doi: 10.1186/s12968-015-0213-2.
19. Truong U, Patel S, Kheyfets V, Dunning J, Fonseca B, Barker AJ, Ivy D, Shandas R, Hunter K. Non-invasive determination by cardiovascular magnetic resonance of right ventricular-vascular coupling in children and adolescents with pulmonary hypertension. *J Cardiovasc Magn Reson*. 2015;17:81. doi: 10.1186/s12968-015-0186-1.
20. Hunter KS, Lee PF, Lanning CJ, Ivy DD, Kirby KS, Claussen LR, Chan KC, Shandas R. Pulmonary vascular input impedance is a combined measure of pulmonary vascular resistance and stiffness and predicts clinical outcomes better than pulmonary vascular resistance alone in pediatric patients with pulmonary hypertension. *Am Heart J*. 2008;155:166–174. doi: 10.1016/j.ahj.2007.08.014.
21. Knight DS, Steeden JA, Moledina S, Jones A, Coghlan JG, Muthurangu V. Left ventricular diastolic dysfunction in pulmonary hypertension predicts functional capacity and clinical worsening: a tissue phase mapping study. *J Cardiovasc Magn Reson*. 2015;17:116. doi: 10.1186/s12968-015-0220-3.
22. Burkett DA, Slorach C, Patel SS, Redington AN, Ivy DD, Mertens L, Younoszai AK, Friedberg MK. Impact of pulmonary hemodynamics and ventricular interdependence on left ventricular diastolic function in children with pulmonary hypertension. *Circ Cardiovasc Imaging*. 2016;9:e004612. doi: 10.1161/CIRCIMAGING.116.004612.
23. Hassoun PM, Mouthon L, Barberà J a., Eddahibi S, Flores SC, Grimminger F, Jones PL, Maitland ML, Michelakis ED, Morrell NW, Newman JH, Rabinovitch M, Schermuly R, Stenmark KR, Voelkel NF, Yuan JXJ, Humbert M. Inflammation, growth factors, and pulmonary vascular remodeling. *J Am Coll Cardiol*. 2009;54:S10–S19.
24. Szulcek R, Happé CM, Rol N, Fontijn RD, Dickhoff C, Hartemink KJ, Grünberg K, Tu L, Timens W, Nossent GD, Paul MA, Leyen TA, Horrevoets AJ, de Man FS, Guignabert C, Yu PB, Vonk-Noordegraaf A, van Nieuw Amerongen GP, Bogaard HJ. Delayed microvascular shear-adaptation in pulmonary arterial hypertension: role of PECAM-1 cleavage. *Am J Respir Crit Care Med*. 2016;33:1–58.
25. Davies PF. Hemodynamic shear stress and the endothelium in cardiovascular pathophysiology. *Nat Clin Pract Cardiovasc Med*. 2009;6:16–26. doi: 10.1038/ncpcardio1397.
26. Guzzardi DG, Barker AJ, van Ooij P, Malaisrie SC, Puthumana JJ, Belke DD, Mewhort HE, Svystonyuk DA, Kang S, Verma S, Collins J, Carr J, Bonow RO, Markl M, Thomas JD, McCarthy PM, Fedak PW. Valve-Related Hemodynamics Mediate Human Bicuspid Aortopathy: Insights From Wall Shear Stress Mapping. *J Am Coll Cardiol*. 2015;66:892–900. doi: 10.1016/j.jacc.2015.06.1310.
27. Cavalcante JL, Lima JA, Redheuil A, Al-Mallah MH. Aortic stiffness: current understanding and future directions. *J Am Coll Cardiol*. 2011;57:1511–1522. doi: 10.1016/j.jacc.2010.12.017.
28. Chesler N, Wang Z. Pulmonary vascular wall stiffness: An important contributor to the increased right ventricular afterload with pulmonary hypertension. *Pulm Circ*. 2011;1:212.
29. Schäfer M, Myers C, Brown RD, Frid MG, Tan W, Hunter K, Stenmark KR. Pulmonary arterial stiffness: toward a new paradigm in pulmonary arterial hypertension pathophysiology and assessment. *Curr Hypertens Rep*. 2016;18:4. doi: 10.1007/s11906-015-0609-2.
30. Nayak KS, Nielsen JF, Bernstein MA, Markl M, D Gatehouse P, M Botnar R, Saloner D, Lorenz C, Wen H, S Hu B, Epstein FH, N Oshinski J, Raman SV. Cardiovascular magnetic resonance phase contrast imaging. *J Cardiovasc Magn Reson*. 2015;17:71. doi: 10.1186/s12968-015-0172-7.
31. Barker AJ, Roldán-Alzate A, Entezari P, Shah SJ, Chesler NC, Wieben O, Markl M, François CJ. Four-dimensional flow assessment of pulmonary artery flow and wall shear stress in adult pulmonary arterial hypertension: results from two institutions. *Magn Reson Med*. 2015;73:1904–1913. doi: 10.1002/mrm.25326.

CLINICAL PERSPECTIVE

The mechanics of the left ventricle and the aorta have been largely understudied in the pathophysiology of pulmonary hypertension in children. In this study, we found increased stiffness—as reflected by pulse wave velocity, aortic strain, and distensibility—by magnetic resonance imaging in the ascending aorta, but not in the descending aorta of these children. The extent of aortic stiffness correlated with the diameter of the main pulmonary artery, suggesting that pulmonary arterial hypertension-related main pulmonary artery dilatation impairs the ability of regions of the ascending aorta to fully expand during systole. Further, aortic stiffness parameters were associated with markers of left ventricular function, including ejection fraction and ventriculo–vascular coupling ratio. This has significant implications on the afterload encountered by left ventricle and may negatively impact left ventricular performance, which is already altered by a sick right ventricle. We surmise that intervention during childhood to improve left-sided ventricular–vascular health may alter disease progression.

Circulation
Cardiovascular Imaging

Apparent Aortic Stiffness in Children With Pulmonary Arterial Hypertension: Existence of Vascular Interdependency?

Michal Schäfer, D. Dunbar Ivy, Steven H. Abman, Alex J. Barker, Lorna P. Browne, Brian Fonseca, Vitaly Kheyfets, Kendall S. Hunter and Uyen Truong

Circ Cardiovasc Imaging. 2017;10:
doi: 10.1161/CIRCIMAGING.116.005817
Circulation: Cardiovascular Imaging is published by the American Heart Association, 7272 Greenville Avenue, Dallas, TX 75231

Print ISSN: 1941-9651. Online ISSN: 1942-0080

Supplemental Material

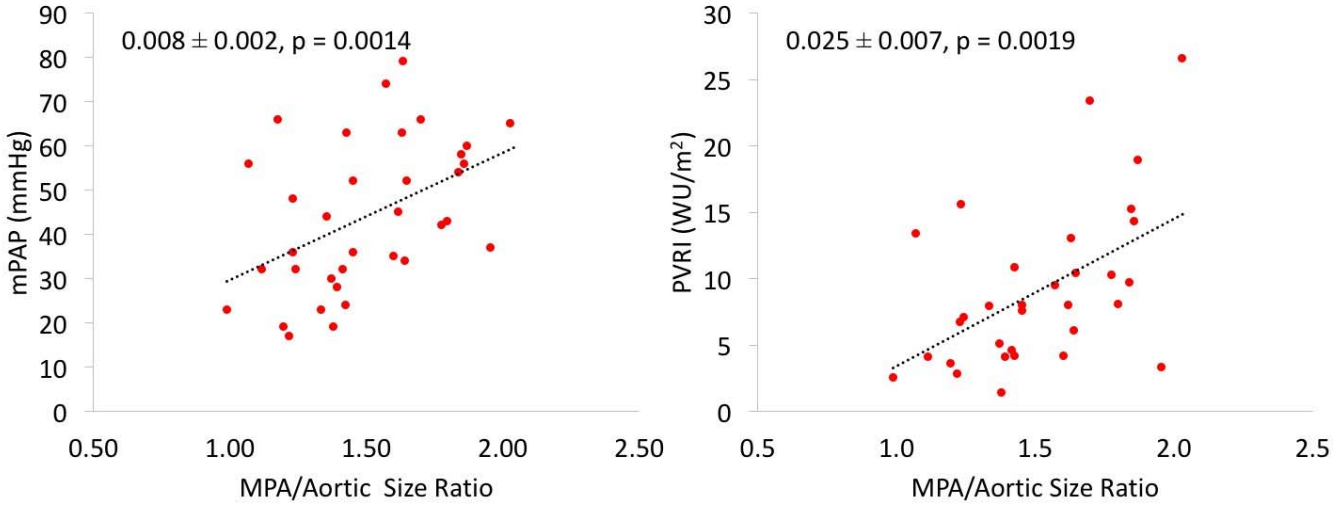

Supplemental Figure. Associations between standard catheterization hemodynamic metrics and MPA to ascending aortic size ratio. As expected, both invasive hemodynamic indices revealed positive correlations with the ratio. We believe that found associations were most likely driven by mean MPA pressure, since it reflects better on local hemodynamic conditions than PVRi. Both correlations were adjusted for age and sex.